Interaction of nebulin SH3 domain with titin PEVK and myopalladin: implications for the signaling and assembly role of titin and nebulin

Kan Ma, Kuan Wang*

Muscle Proteomics and Nanotechnology Section, Laboratory of Muscle Biology, B50/Rm 1140, National Institute of Arthritis and Musculoskeletal and Skin Diseases, National Institutes of Health, Bethesda, MD 20892, USA

Received 14 August 2002; revised 23 October 2002; accepted 26 October 2002

First published online 15 November 2002

Edited by Amy McGough

Abstract **Skeletal muscle nebulin is thought to determine thin filament length and regulate actomyosin interaction in a calcium/calmodulin or S100 sensitive manner. We have investigated the binding of nebulin SH3 with proline-rich peptides derived from the 28-mer PEVK modules of titin and the Z-line protein myopalladin, using fluorescence, circular dichroism and nuclear magnetic resonance techniques. Of the six peptides studied, PR2 of titin (VPEKKAPVAPPK) and myopalladin MyoP2 (^{646}VKEPPPVLAKPK^{657}) bind to nebulin SH3 with micromolar affinity (~31 and 3.4 μM, respectively), whereas the other four peptides bind weakly (>100 μM). Sequence analysis of titins reveals numerous SH3 binding motifs that are highly enriched in the PEVK segments of titin isoforms. Our findings suggest that titin PEVK and myopalladin may play signaling roles in targeting and orientating nebulin to the Z-line during sarcomere assembly.**

Key words: Circular dichroism; Nuclear magnetic resonance; Fluorescence; SH3 domain of nebulin; Myopalladin; PEVK

1. Introduction

The Src homology-3 (SH3) domain, a family of small globular domains of 60 amino acids, serves as a mediator of protein–protein interactions in signaling pathways [1]. It has a hydrophobic cleft formed by two orthogonal β-sheets that binds polyproline type II helices with a core binding motif PxxP [2]. Structural studies of SH3 domain–ligand complexes have led to a general model for SH3–ligand interactions and identified two classes of SH3 ligands that bind SH3 domains in opposite orientations: class I, with the consensus sequence RxxPxxP, and class II, with the consensus sequence xPxxPxR [3].

Nebulin, which consists of an acidic N-terminal domain, 35 residue module repeats, a linker domain and a C-terminal SH3 domain, is thought to determine thin filament length of skeletal muscle and regulate actomyosin interaction in a calcium/calmodulin or S100 sensitive manner [4–7]. The C-terminal SH3 domain of nebulin (nSH3) is anchored at the Z-line and thus orients and aligns the ~1 μm long molecule along the length of the thin filaments [8–11]. The presence of a SH3 domain at the C-terminus of nebulin (700–800 kDa) as well as the heart specific analog nebulette (107 kDa) and in the recently discovered giant protein obscurin (721 kDa) [12,13] in striated muscle sarcomeres has led to the search for SH3 receptors in the sarcomere. Since nuclear magnetic resonance (NMR) investigations have indicated that the nebulin SH3 domain folds as a typical all-β SH3 fold [14], one expects proteins with polyproline II helices to be prime targets. Politou et al. [14] speculated that the sequence, TPPRIPPKKP, of human cardiac titin Z domains is a likely candidate. We have observed that cloned human fetal nSH3 binds actin, tropomyosin and troponin in solid-state assays [7]. Recently, myopalladin (145 kDa) has been identified as a receptor that simultaneously links nebulin SH3 and α-actinin in the Z-line. One PPP-containing peptide of myopalladin was identified as a binding site by yeast two-hybrid screening of mutagenized constructs [15].

Titin is a family of giant elastic proteins (3–4 MDa) that consists of serially linked motifs of three types: the folded 100 residue modular repeats of immunoglobin or fibronectin domains, a unique PEVK motif and the N2-A or N2-B insert [16]. The notion that the PEVK region of titin may contain numerous SH3 recognition sites was prompted by our search for six common SH3 binding motifs in titin isoforms that revealed a surprisingly large number of these motifs, with class I and II being the most abundant and enriched in the PEVK regions.

Experimentally, we have demonstrated by circular dichroism (CD), fluorescence spectroscopy and NMR techniques the binding of the nSH3 to proline-rich peptides of myopalladin and the PEVK segment of titin that conform to the canonical consensus sequences for SH3 binding peptides. We report that myopalladin MyoP2, with a PPP motif, and PR2, which conforms to both the class I and class II motifs, bind to nSH3 with micromolar affinity (~31 and 3.4 μM, respectively), whereas the other four peptides bind weakly (>100 μM). These observations pose an intriguing functional implication of titin PEVK segments and Z-line SH3 binding proteins such

*Corresponding author. Fax: (1)-301-402 8566.
E-mail address: wangk@exchange.nih.gov (K. Wang).

Abbreviations: HSQC, heteronuclear single quantum coherence; MyoP1, MyoP2, MyoP3, peptide fragments of myopalladin; MALDI-TOF, matrix-assisted laser desorption ionization time of flight; PPII, polyproline type II left-handed helix; PR, a 28-mer sequence module of PEVK; PR1, PR2, PR3, subfragments of PR; Sos, SH3 binding sequence of guanine nucleotide exchange factor

0014-5793/02/$22.00 © 2002 Published by Elsevier Science B.V. on behalf of the Federation of European Biochemical Societies.
PII: S0014-5793(02)03655-4

as myopalladin for the nebulin targeting pathway during the IZI assembly.

2. Materials and methods

2.1. Search for SH3 binding motifs

The search for SH3 binding motifs on myopalladin and titin/PEVK isoforms was performed using Protein Subsequence within MacVector (version 98) for: PxxP [2], KxxPxxP [3], xPxxPxK [3], xPxxxxPV(A)xP [2], PxxxKxxKP [17] and PxxDY [18].

Myopalladin (EMBL, AF328296, residues 1–1320), human fetal skeletal PEVK (GenBank, AF321609, residues 1–786), human cardiac titin PEVK (SwissProt, Q10466, residues 1–186) and human soleus PEVK (GenBank, CAD12456, residues 1–2154) were included in this search.

2.2. Expression and purification of the nebulin SH3 domain

The soluble nSH3 (accession number AAB02622) was expressed using Bl21(DE3)pLysS host cells transfected with a pET3d plasmid (Novagen, Madison, WI, USA) in LB medium and purified as described previously [7].

The ^{15}N-labeled nSH3 was prepared by growing the bacteria in M9 minimal medium with $^{15}NH_4Cl$ as a sole nitrogen source during the expression. The incorporation of ^{15}N labels was confirmed by matrix-assisted laser desorption ionization time of flight (MALDI-TOF) mass spectroscopy (as a mass increase of 73.6) and heteronuclear NMR spectroscopy. The folding of the nSH3 was monitored by CD and thermal titration from 2 to 80°C. It is completely unfolded at 60°C, consistent with the reported value [14].

2.3. Peptide synthesis and purification

A 28 residue titin PEVK (accession number AF321609) module (PEPPKEVVPEKKAPVAPPKKPEVPPVKV) (PR), including three fragments: PR1 (KVPEPPKEVVPE), PR2 (VPEKKAPVAPPK) and PR3 (KPEVPPVKV), was synthesized and purified as described elsewhere [19]. Three 12-mer myopalladin (accession number AF328296) peptides, MyoP1 (^{638}KTPEPSSPVKEP^{649}), MyoP2 (^{646}VKEPPPVLAKPK^{657}) and MyoP3 (^{570}VEQPPKPKIEGV^{581}), were synthesized by Sigma Genosys. Human SH3 binding sequence of guanine nucleotide exchange factor (hSos) SH3 binding domain (^{1149}VPPPVPPRRR^{1158}) was purchased from Calbiochem. The purity of the peptides (>98%) was confirmed by analytical high performance liquid chromatography and MALDI-TOF.

2.4. Fluorescence spectroscopy

Fluorescence measurements were carried out with an Aminco-Bowman Series 2 spectrofluorometer at 2, 10 and 22°C. The excitation wavelength was 280 nm (4 nm slit), and the emission wavelength was 350 nm. In a peptide titration assay, aliquots of peptide solutions in water (Sos: 0.85 mM, PR: 7.1 mM, PR1: 6.9 mM, PR2: 2.5 mM, PR3: 11 mM, MyoP1: 6.8 mM, MyoP2: 2.5 mM and MyoP3: 6.7 mM) were added to 2.5 ml of SH3 solution (5 μM) in 10 mM KPi, pH 6.7, and the mixture was stirred in a cuvette for 2–5 min prior to use. To measure the dissociation constant (K_d), peptide aliquots were added until no significant SH3 dependent changes in fluorescence intensity and maximum wavelength were observed. Binding constants were calculated from the isotherms assuming a 1:1 stoichiometry with Simfit (version 5.40, University of Manchester, UK).

2.5. CD spectroscopy

All spectra were obtained with a Jasco spectropolarimeter, model J-715, installed with a standard data analysis program and a Peltier type temperature control system (Jasco, Tokyo, Japan). The far-UV spectra were recorded in the range of 190–250 nm with a 0.1 cm path length cuvette in 10 mM KPi buffer at pH 6.7.

2.6. NMR spectroscopy

NMR samples were prepared by dialyzing proteins against 50 mM NaCl, 10 mM NaPi, pH 7.0. The final protein concentration was ~0.4 mM in H_2O/D_2O (9/1). All experiments were acquired with Varian Unity-Plus 600 MHz spectrometer using a triple resonance probe at 25°C. Changes in ^{15}N and ^{1}H chemical shift were monitored by two-dimensional heteronuclear single quantum coherence (2D-HSQC) experiments. The titration was stopped when there were no further chemical shift changes upon addition of the peptide. All NMR data were processed with Felix (MSI). A tentative assignment was done by comparing the recently published data on a 60 residue human adult nebulin SH3 [20]. Our 58 residue human fetal nSH3 is of identical sequence, but two residues shorter at the N-terminus.

3. Results

3.1. Multiple SH3 binding motifs in titin PEVK isoforms

Our initial survey of six types of SH3 binding motifs (PxxP [2], class I KxxPxxP [3], class II xPxxPxK [3], xPxxxxPV(A)xP [2], PxxxKxxKP [17], and PxxDY [18]) in titin and PEVK sequences from several species revealed an unexpectedly large number of these motifs that are significantly enriched in PEVK segments. Table 1 presents the total number of hits per sequence. The core PxxP motif is abundant in titin, with 69, 113, and 7 copies in the PEVK segments of human fetal skeletal, human soleus and cardiac titins. Since the core motif as such is undoubtedly too short to be useful in identifying SH3 binding sites, we have focused our analysis on the search for class I and II motifs, two well established SH3 binding motifs of seven residues each. There are 11, 17, and one copies of the class I motif and 14, 30, and 1 copies of the class II motif in the PEVK segments of human fetal skeletal, human soleus and cardiac titins, respectively.

The distributions of class I and II motifs along the length of the titin sequences are plotted in Fig. 1, illustrating the striking enrichment of these motifs in the PEVK segments of titin isoforms. In general, it is noted that these motifs are evenly distributed along the A-band region of the titin. In contrast, the motifs in the I-band are nearly exclusively found in the PEVK region, with the remainder of the I-band and the Z-lines (titin N-terminus) almost free of such motifs. This segmentation of multiple SH3 binding motifs along the sarcomere is striking, and suggests the potential roles for signaling events in this region.

Table 1
SH3 binding motifs in titin/PEVK isoforms

SH3 binding motif	Human fetal skeletal titin (hits)		Human soleus titin (hits)		Human cardiac titin (hits)	
	PEVK (786)	Titin (N/A)	PEVK (2154)	Titin (34 350)	PEVK (186)	Titin (26 926)
PxxP	69	–	113	417	7	310
Class I[a]						
KxxPxxP	11	–	17	27	1	12
Class II[a]						
xPxxPxK	14	–	30	62	1	35
xPxxxxPV(A)xP	5	–	8	9	0	1
PxxxKxxKP	0	–	0	2	0	1
PxxDY	0	–	1	5	0	3

[a]Some sequences can be classified as both class I and II motifs.

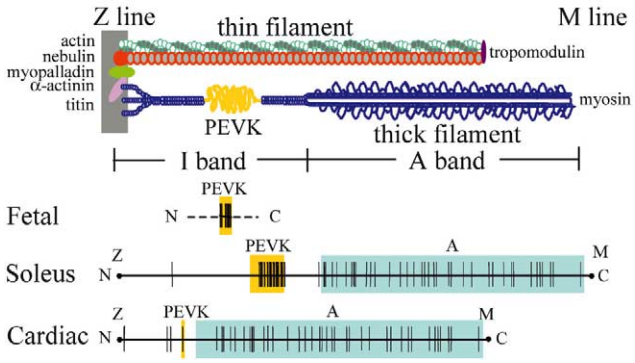

Fig. 1. Sarcomere proteins and distribution of class I and class II SH3 binding motifs along the sequence of titin isoforms. A schematic diagram of a half sarcomere showing the Z-line attachment of actin (dark green), nebulin (red), myopalladin (green), α-actinin (pink), and titin (blue). The C-terminal SH3 domain of nebulin is shown as a solid red circle and the titin PEVK as a yellow string. Tropomodulin (purple) and myosin (gray and blue) are also shown. The distribution of class I and class II SH3 binding motifs is shown as vertical bars along three titin isoforms: human fetal titin (partial, AF321609), human soleus titin (CAD12456) and human cardiac titin (I38344). Titin PEVK and A-band segments are shaded in yellow and cyan, respectively.

3.2. Interaction between nebulin SH3 and PEVK peptides

The potential interaction of these SH3 binding motifs is being evaluated systematically with synthetic peptides and biophysical methods. Since the intrinsic fluorescence of tryptophan and other aromatic residues at the ligand binding site provides a sensitive binding assay, we first tested the binding by adding saturating concentrations of PR, PR1, PR2, and PR3 to the nSH3 solutions. We also studied in parallel the proline-rich VPPPVPPRRR decapeptide derived from Sos as a control peptide because of its high affinity for the N-terminal SH3 domain of Grb2 [21]. In the presence of Sos, PR and PR2 peptides, there is an increase in the Trp fluorescence intensity and a blue shift of its maximum at 339 nm for free nSH3, to 331 nm (nSH3-Sos), 333 nm (nSH3-PR) and 335 nm (nSH3-PR2) (Fig. 2A). These data suggest that the active site Trp is moved to an increasingly non-polar environment upon binding of peptides [22]. This conformational change of nSH3 increases in the order PR2, PR and Sos, as revealed by the relative increase of fluorescence intensity and the magnitude of blue shift. Titration of nSH3 with peptides yielded dissociation constants of 2.3 μM for Sos, 29 μM for PR and 77 μM for PR2 for a 1:1 stoichiometry at 22°C (Fig. 2B,C). In contrast, the addition of PR1 and PR3 to nSH3 caused the fluorescence intensity to decrease slightly without affecting its maximum (data not shown), suggesting little contact between PR1, PR3 and the aromatic cleft of the nSH3 domain.

Interestingly, the fluorescence intensity of the nSH3 at 2°C is approximately two-fold higher than at 22°C (Fig. 2B,C), indicating more exposure of the Trp residue at higher temperature. Titration of nSH3 with Sos, PR and PR2 at both temperatures demonstrated lower dissociation constants and tighter binding for these peptides at 2°C than at 22°C. The increased binding affinity at 2°C may be contributed by both the conformational changes of nSH3 and a stabilization of the polyproline type II left-handed (PPII) helices in PEVK peptides at this lower temperature (Ma and Wang, unpublished observation).

The far-UV CD spectra were then measured to assess if the binding induces conformational changes in the polypeptide bonds. The CD of the nSH3–Sos mixture showed a noticeable intensity increase and a slight blue shift of the negative band from 201 to 199 nm, as compared to the sum of individual spectra (Fig. 3A). This may arise from a net increase in either PPII structure (Ma and Wang, unpublished observation) or alternatively, the unordered structure [23]. The spectra for nSH3–PR2 displayed a small, but easily measured increase near 222 nm, without major changes in the negative band near 200 nm (Fig. 3B). The increase around 222 nm may result from the environmental change of the aromatic residues present in nSH3, in analogy with the spectral changes upon binding of Fyn–SH3 to 3BP1 and 3BP2 peptides [23]. Titration of nSH3 with PR2 yielded a dissociation constant of 24 μM for nSH3–PR2 complex at 2°C (Fig. 3C), consistent with the K_d of 31 μM derived from fluorescence titration (Fig. 2C). The nSH3–PR/PR2 interactions are also slightly sensitive to ionic strength, with dissociation constants reduced about two-fold at 150 mM KCl, 10 mM KPi at 22°C (data not shown).

3.3. nSH3 and myopalladin peptides interaction

Bang et al. [15] reported based on yeast two-hybrid assays that myopalladin binds to nebulin SH3 at the Z-line via ^{646}VKEPPPVLAKPK^{657} (designated as MyoP2 here), one of the three proline-rich motifs near the middle of the 145 kDa protein. The other two SH3 motifs, ^{638}KTPEPSSPVKEP^{649}

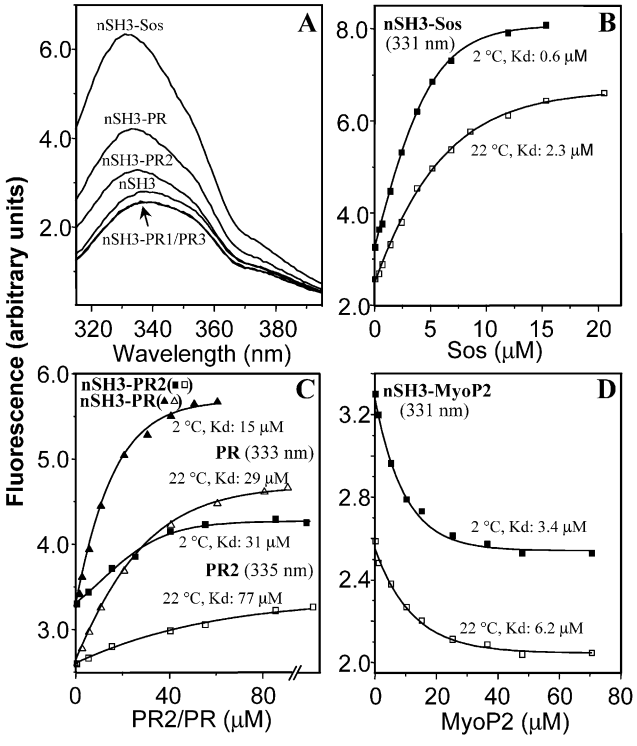

Fig. 2. Fluorescence titration of the interaction of nebulin SH3 with Sos, PEVK and myopalladin peptides. A: Fluorescence spectra of nSH3 and nSH3–peptide complexes. nSH3 (0.9 μM) and peptides (Sos: 6.5 μM, PR: 19 μM, PR1: 39 μM, PR2: 43 μM and PR3: 63 μM) were in 10 mM KPi, pH 6.7 at 10°C. B–D: Binding isotherms of nSH3-Sos (B), nSH3-PR and nSH3-PR2 (C), and nSH3-MyoP2 (D). nSH3 (5 μM in 10 mM KPi, pH 6.7) was titrated with each peptide at 2°C (closed symbols) and 22°C (open symbols). The fluorescence intensity at 331 nm (Sos and MyoP2), 333 nm (PR) and 335 nm (PR2) was plotted as a function of total ligand concentrations.

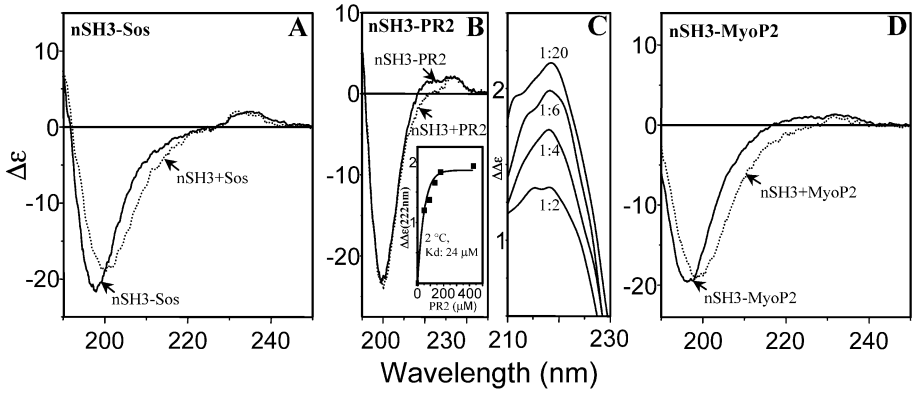

Fig. 3. CD titration for nSH3 with Sos, PR2 and MyoP2. nSH3 (21 μM in 10 mM KPi at pH 6.7) was titrated with peptides at 22°C (A) and 2°C (B–D). The spectra of the mixtures are labeled with 'nSH3–Sos', 'nSH3–PR2', 'nSH3–MyoP2' and the sums of individual spectra of nSH3 and free peptides are labeled as 'nSH3+Sos', 'nSH3+PR2', 'nSH3+MyoP2', respectively. Difference CD spectra of PR2 titration with increasing PR2/nSH3 molar ratios are shown in (C). The binding isotherm of nSH3-PR2 is plotted based on the difference ellipticity at 222 nm as a function of total peptide concentration (B, inset).

(as MyoP1) and ^{570}VEQPPKPKIEGV^{581} (as MyoP3), were excluded by deletion and competition binding assays. We evaluated the SH3 binding affinity of these motifs by direct binding assays. Fluorescence titration of nSH3 with MyoP1, MyoP2 and MyoP3 indicated that all three peptides bind to nSH3, with two distinct sets of affinities and conformations. The emission maximum of MyoP2/nSH3 shifted from 339 nm to 331 nm and MyoP1 and MyoP3 caused the maxima to blue shift from 339 nm to 335 nm (MyoP1) and 333 nm (MyoP3). The binding isotherms for MyoP2 were fit well with a single site binding model, yielding K_ds of 3.4 μM and 6.2 μM for 2°C and 22°C, respectively (Fig. 2D). In contrast, the isotherms for MyoP1 and MyoP3 showed no saturation up to 300 μM and displayed a slight sigmoidal shape, indicating a very different mode of interaction and much weaker binding.

It is significant that this micromolar affinity between nSH3 and the MyoP2 peptide is also manifested in vivo [15]. On the other hand, the class II or PxxP containing peptides (MyoP1 and MyoP3) interact very weakly with nSH3 and no binding was detectable in vivo [15]. It is noteworthy that, contrary to an enhancement upon binding of Sos and PR2 to nSH3, the addition of MyoP2 was accompanied by a progressive quenching of Trp fluorescence at 350 nm. This may have resulted from a more efficient energy transfer between Trp and one or more Tyr residues in the binding site. A similar quenching of SH3 fluorescence upon ligand binding was reported for Y7V-Grb2-N-SH3 [24].

In contrast to such distinct changes of the Trp environment, the far-UV CD spectra of nSH3-Sos (Fig. 3A) and nSH3-MyoP2 (Fig. 3D) are very similar, suggesting the same net changes in polypeptide backbone conformations upon ligand binding.

3.4. Interfaces of nSH3–Sos and nSH3–PR2 complexes

Since the change in chemical shifts of protein resonances upon ligand binding is a sensitive method for defining the protein interface [25], we also measured the interaction of nSH3 with Sos and PEVK peptides using HSQC techniques. As shown in the HSQC spectra of ^{15}N isotope enriched nSH3 (Fig. 4), the number of NMR signals is consistent with the number of labeled backbone and side chain nitrogen atoms of nSH3. However, some lower intensity crosspeaks are observed indicating that additional conformations exist in minor amounts. Titration of nSH3 with Sos caused increasing chemical shift changes of Trp36 (with indolic NH at 9.95 ppm), Glu35, Ala15, Asp16, Glu34, Met11 and Tyr54 (arrows in Fig. 4A), all of which are known to be involved in the ligand–SH3 interface [24]. Minor changes were also observed

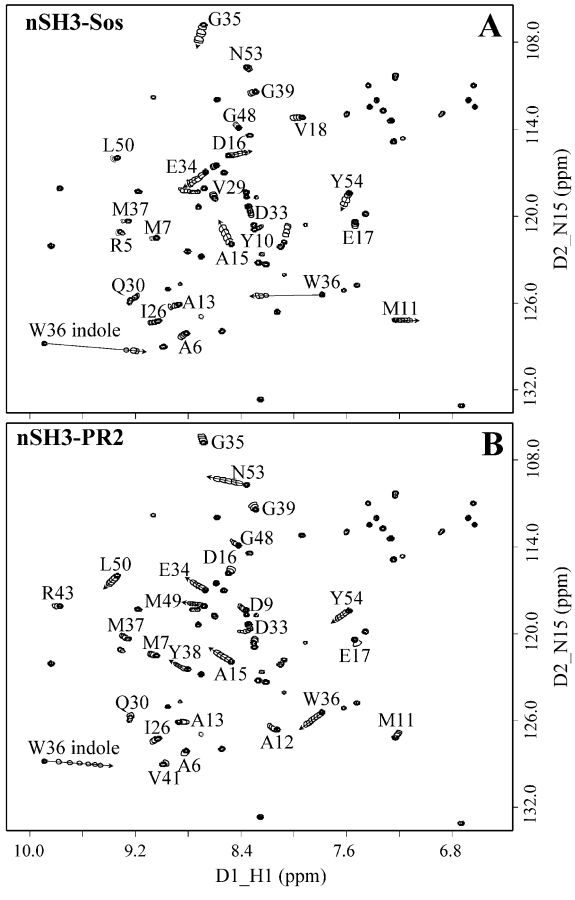

Fig. 4. 2D ^{1}H–^{15}N HSQC titration of nSH3 with Sos and PR2. The HSQC spectra were recorded on a 0.37 mM solution of uniformly ^{15}N-labeled nSH3 in 50 mM NaCl, 10 mM NaPi, pH 7.0 (90% H_2O/10% D_2O) at 25°C and then titrated with 9 increments of Sos up to 0.34 mM or 11 increments of PR2 up to 1.36 mM. The major chemical shift changes for affected residues are plotted as a series of circles on each arrow.

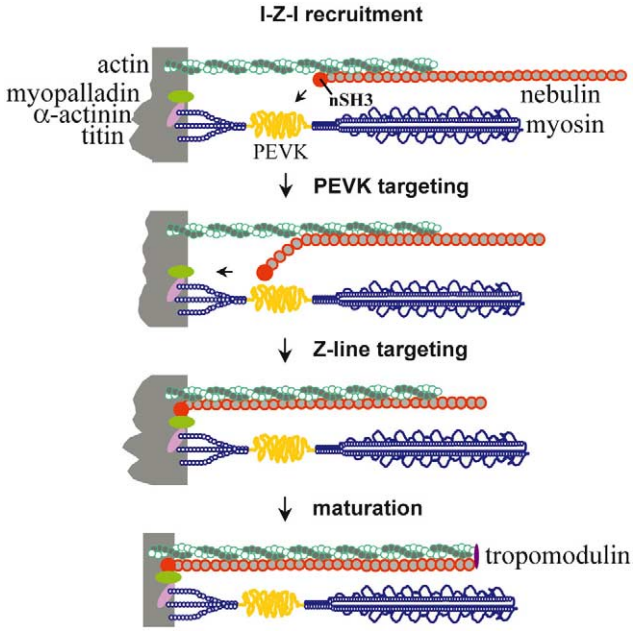

Fig. 5. A hypothetical model of nebulin targeting pathway during IZI assembly. In this model, both the binding of nebulin modules to actin thin filaments (IZI recruitment) and the concurrent or sequential binding of nebulin C-terminal SH3 to the multiple binding sites in the PEVK segment (PEVK targeting) serve to recruit and orient a large number of nebulin molecules to the IZI complexes [7]. The Z-line maturation process may commence when nebulin relocates to the Z-lines by binding or sliding its SH3 toward myopalladin, α-actinin and actin in the Z-line (Z-line targeting). Finally, the maturation of the Z-line to form a sharp and regularly aligned lattice and the attachment of tropomodulin to the pointed end of the actin and nebulin filaments, in turn, transform the actin/troponin/tropomyosin/nebulin containing composite thin filaments into the mature IZI complexes with uniform length and precise lateral registration. Irregular and diffuse Z-bands are transformed into sharp and narrow Z-lines as a result of the maturation process. Color scheme as in Fig. 1.

for other residues (Fig. 4A). These residues are located either adjacent (Asn53, Asp33, Tyr10, Glu17, Ala13, Met7 and Met37) or outside (Gly39, Gly48, Val18, Leu50, Val29, Ile26, Ala6, Gln30 and Arg5) of the pocket, suggesting a ligand induced conformational change of nSH3. Overall, our data are consistent with the NMR study of Grb2/SH3–Sos complex [24].

Titration of nSH3 with PR2 and PR perturbed the chemical shift of a same set of residues: Asn53, Leu50, Met49, Trp36, Glu34, Ala15, Tyr38 and Tyr54 (Fig. 4B). These residues are located in or close to the conserved hydrophobic pocket of the nSH3 [14]. Further comparison of the HSQC perturbation spectra of nSH3–PR/PR2 with those of nSH3–Sos showed highly similar but non-identical chemical shift changes (Fig. 4). The distinct changes of chemical shifts for Asn53, Leu50, Met49 and Tyr38 in nSH3–PR/PR2 as compared to changes in Glu35, Asp36 and Met11 in nSH3–Sos probably reflect the unique effect of the PPP motif in Sos on the conformation near the nSH3 binding cleft.

4. Discussion

Our search for six common SH3 binding motifs in titin isoforms revealed a large number of SH3 motifs, with class I and II motifs being the most abundant. The distribution of class I and II motifs along the sequences of titin revealed a significant enrichment of these motifs in the PEVK segments of titin isoforms. It is noted that these motifs are fairly evenly distributed along the A-band region of titin. In contrast, the motifs in the I-band are almost exclusively found in the PEVK region, with the remainder of the I-band and the Z-line (titin N-terminal) regions free of such motifs. This segmentation of multiple SH3 binding motifs along the sarcomere is striking, and suggests a potential signaling role of SH3 proteins in A-band and I-band assembly, turnover and contractile activities.

That these PEVK motifs indeed bind to SH3 is supported by our demonstration of nebulin SH3 binding to PR/PR2 peptides of a highly repetitive motif from human fetal PEVK (exon 172 of the human titin gene [13]). The PR2 in the center of the 28 residue PEVK module contains a SH3 binding motif sequence (KxxPxxPxK) with APVAP forming a polyproline II left-handed helix in solution [19]. Our conformational studies indicate that PR2 binds to the hydrophobic pocket of nSH3 in a manner that is shared among SH3 and polyproline peptides [1]. PR1 and PR3, representing the flanking regions of PR2, do not by themselves bind to nSH3, despite the presence of a short PPII helix in each peptide [19]. These flanking regions, however, enhance the overall affinity of PR towards nSH3 at least two-fold (from 77 μM of PR2 to 29 μM of PR at 22°C) (Fig. 2C), suggesting the possibility of stabilization of PPII in PR2 by flanking regions of this module or additional interaction outside the hydrophobic pocket of nSH3. Given the high sequence homology of PEVK exons [13], it is reasonable to assume that each of the SH3 binding motifs in most PEVK exons also binds SH3. Thus the PEVK segments of skeletal muscle titins, produced by differential splicing to incorporate selected PEVK exons, are likely to contain tandem repeats of SH3 binding sites along their length. Such a multivalent lattice-like receptor is likely to bind SH3 containing proteins with an avidity that is significantly higher than the affinity of each individual site.

The biological significance of the PEVK/SH3 interaction remains to be established. Many important SH3 mediated biological interactions arise from ligand interactions with micromolar affinity that manifests in a milieu of high local protein concentrations [1]. Taking into consideration the fact that the protein concentration of major sarcomere proteins is in the mM range [26], it is reasonable to expect that both titin PEVK and nebulin SH3 domain may participate in signaling pathways by interacting with other SH3 receptors and multiple polyproline ligands at various stages of muscle development.

Our previous myofibril assembly studies indicated that even though nebulin was expressed early in developing skeletal muscle culture, it started to participate in myofibrillar assembly only at a late stage during the maturation of preformed IZI complexes when the thin filaments became uniform in length and aligned across the sharp Z-lines [27]. We proposed that nebulin acts as a molecular ruler in restricting the length of preformed actin filaments by stabilizing the actin filaments at uniform length [27]. How this giant protein is recruited to the immature sarcomere and how it orients its C-terminal SH3 toward the Z-lines are still unclear. The maturation process may commence when nebulin is attached to actin filaments and becomes oriented with the same polarity and then attached at its C-terminus to the Z-lines [28]. Our current find-

ing that nSH3 is capable of binding both to multiple sites along the length of PEVK segments and to myopalladin suggests that titin PEVK may serve to coordinate and expedite this orientation and maturation process (see Fig. 5). If this is true, then titin PEVK represents a new signaling segment that is distinct from the titin domains that are implicated in the regulation of ion channels, protein turnover and gene expression (reviewed in [29]).

Acknowledgements: We thank Ms. Wanxia Li for the preparation of ^{15}N-labeled and non-labeled nebulin SH3. We also thank the Cleveland Center for Structural Biology for the use of NMR spectrometer.

References

[1] Mayer, B.J. (2001) J. Cell Sci. 114, 1253–1263.
[2] Ren, R., Mayer, B.J., Cicchetti, P. and Baltimore, D. (1993) Science 259, 1157–1161.
[3] Feng, S., Chen, J.K., Yu, H., Simon, J.A. and Schreiber, S.L. (1994) Science 266, 1241–1247.
[4] Kruger, M., Wright, J. and Wang, K. (1991) J. Cell Biol. 115, 97–107.
[5] Labeit, S., Gibson, T., Lakey, A., Leonard, K., Zeviani, M., Knight, P., Wardale, J. and Trinick, J. (1991) FEBS Lett. 282, 313–316.
[6] Labeit, S. and Kolmerer, B. (1995) J. Mol. Biol. 248, 308–315.
[7] Wang, K., Knipfer, M., Huang, Q.Q., van Heerden, A., Hsu, L.C., Gutierrez, G., Quian, X.L. and Stedman, H. (1996) J. Biol. Chem. 271, 4304–4314.
[8] Wang, K. and Wright, J. (1988) J. Cell Biol. 107, 2199–2212.
[9] Wright, J., Huang, Q.Q. and Wang, K. (1993) J. Muscle Res. Cell Motil. 14, 476–483.
[10] Young, P., Ferguson, C., Bauelos, S. and Gautel, M. (1998) EMBO J. 17, 1614–1624.
[11] Millevoi, S., Trombitas, K., Kolmerer, B., Kostin, S., Schaper, J., Pelin, K., Granzier, H. and Labeit, S. (1998) J. Mol. Biol. 282, 111–123.
[12] Young, P., Ehler, E. and Gautel, M. (2001) J. Cell Biol. 154, 123–136.
[13] Bang, M.L. et al. (2001) Circ. Res. 89, 1065–1072.
[14] Politou, A.S., Millevoi, S., Gautel, M., Kolmerer, B. and Pastore, A. (1998) J. Mol. Biol. 276, 189–202.
[15] Bang, M.L. et al. (2001) J. Cell Biol. 153, 413–427.
[16] Labeit, S. and Kolmerer, B. (1995) Science 270, 293–296.
[17] Kato, M., Miyazawa, K. and Kitamura, N. (2000) J. Biol. Chem. 275, 37481–37487.
[18] Mongiovi, A.M., Romano, P.R., Panni, S., Mendoza, M., Wong, W.T., Musacchio, A., Cesareni, G. and Fiore, P.P.D. (1999) EMBO J. 18, 5300–5309.
[19] Ma, K., Kan, L. and Wang, K. (2001) Biochemistry 40, 3427–3438.
[20] Politou, A.S. et al. (2002) J. Mol. Biol. 316, 305–315.
[21] Wittekind, M., Mapelli, C., Lee, V., Goldfarb, V., Friedrichs, M.S., Meyers, C.A. and Mueller, L. (1997) J. Mol. Biol. 267, 933–952.
[22] Ross, J.B., Szabo, A.G. and Hogue, C.W. (1997) Methods Enzymol. 278, 151–190.
[23] Viguera, A.R., Arrondo, J.L., Musacchio, A., Saraste, M. and Serrano, L. (1994) Biochemistry 33, 10925–10933.
[24] Vidal, M., Goudreau, N., Cornille, F., Cussac, D., Gincel, E. and Garbay, C. (1999) J. Mol. Biol. 290, 717–730.
[25] Otting, G., Qian, Y.Q., Billeter, M., Müller, M., Affolter, M., Gehring, W.J. and Wüthrich, K. (1990) EMBO J. 9, 3085–3092.
[26] Squire, J. (1986) Muscle: Design, Diversity, and Disease, Benjamin/Cummings, Menlo Park, CA.
[27] Moncman, C.L. and Wang, K. (1996) Cell Motil. Cytoskel. 34, 167–184.
[28] Moncman, C.L. and Wang, K. (1999) Cell Motil. Cytoskel. 44, 1–22.
[29] Granzier, H. and Labeit, S. (2002) J. Physiol. 541, 335–342.